MODELING ANISOTROPIC CONDUCTIVITY BEHAVIOR OF SiCp/Al METAL-MATRIX COMPOSITE EXTRUSIONS

P. K. Liaw
Westinghouse Science & Technology Center
Pittsburgh, PA 15235

R. Pitchumani and S. C. Yao
Department of Mechanical Engineering
Carnegie Mellon University
Pittsburgh, PA 15213

D. K. Hsu, B. Foster and H. Jeong*
Center for Nondestructive Evaluation
Iowa State University
Ames, IA 50011

INTRODUCTION

Metal-matrix composites (MMCs) appear to be well suited for structural applications where high specific strength (strength-to-density ratio), high specific modulus (modulus-to-density ratio) and high-temperature material properties provide significant engineering and economic advantages. So far, relatively little work was conducted on nondestructive characterization of MMCs [1-5]. The main goal of this paper was to investigate the use of the nondestructive eddy current technique for the evaluation of the electrical conductivity behavior of silicon-carbide-particulate (SiC_p) reinforced aluminum (Al) MMCs, and to develop theoretical models to predict the results.

EXPERIMENTAL PROCEDURES

SiC_p reinforced Al MMCs extruded plates were purchased from DWA Composite Specialties, Inc. These materials were fabricated by the powder metallurgy (P/M) technique.

*Now at Agency for Defense Development, DaeJon, Korea

Review of Progress in Quantitative Nondestructive Evaluation, Vol. 12
Edited by D.O. Thompson and D.E. Chimenti, Plenum Press, New York, 1993

The Al base alloys were 2124, 6061 and 7091, and the volume percentages (v/o) of SiC_p reinforcement covered a wide range of 0, 10, 20, 25, 30, 40 and 55%. The composite materials were received in an extruded-plate form with the final extrusion ratios ranging from 11:1 to 39:1. Figure 1(a) presents the orientation of the composite extrusions, where x_1 is the extrusion direction, x_2 is the in-plane transverse direction, and x_3 is the out-of-plane thickness direction. Furthermore, the x_1-x_2 plane is the extrusion plane, and both x_1-x_3 and x_2-x_3 planes are perpendicular to the extrusion plane. The experimental procedure consisted of preparing metallographic specimens for the microstructural characterization of the x_1-x_2, x_1-x_3 and x_2-x_3 planes, respectively [Figure 1(a)], using scanning electron microscopy (SEM).

Eddy current measurements were made using a Nortec NDT-16 eddyscope and a 10 kHz (SP-10A) probe. The samples were parallelepipeds machined from the extruded plates, and their faces made parallel to the symmetry planes (x_1-x_2, x_1-x_3 and x_2-x_3 planes), shown in Figure 1(a). A calibration curve was first established to relate the eddyscope output voltage of the "lift-off" signal to the electrical conductivity in units of percent IACS (International Annealed Copper Standard). Because of the circular symmetry of the eddy current coil, the measurements yielded planar conductivity that was an average of the conductivities along different directions on the plane. Measurements were made on the x_1-x_2, x_1-x_3, and x_2-x_3 planes to determine their respective planar conductivities.

RESULTS

The average size of SiC_p varied from approximately 2 to 4 μm for each series of composite system (2124, 6061 or 7091 Al MMCs). The aspect ratio of SiC_p ranged from approximately 2 to 3. Figure 1 shows the example microstructural features of a typical extruded product [7091/SiC/30p, where 7091 is the Al base (matrix) alloy, SiC is the silicon-carbide reinforcement, and 30p is the thirty volume percentage of particulate reinforcement] on the three symmetry planes.

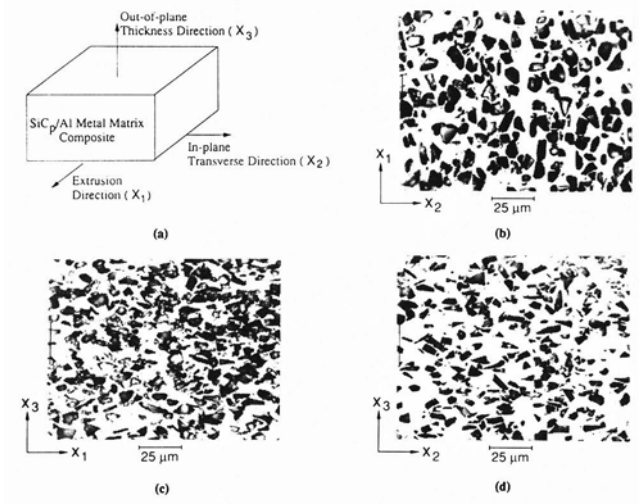

Figure 1. (a) Schematic of a SiC_p composite extrusion showing three symmetry axes, (b) - (d) Micrographs of a 7091/SiC/30p composite on the x_1-x_2, x_1-x_3 and x_2-x_3 planes, respectively.

In Figure 1, the micrographs of the cross sections of the composite along the three symmetry planes reveal that the SiC_p cross sections are flat and nearly rectangular in shape on the x_1-x_2 plane [Figure 1(b)], while observed on the x_1-x_3 and x_2-x_3 planes, they are elongated and approximately elliptical and narrow-rectangular in shape [Figures 1(c) and 1(d), respectively]. Moreover, on the x_1-x_3 and x_2-x_3 planes [Figures 1(c) and 1(d)], SiC_p is randomly distributed, but preferentially oriented in the extrusion (x_1) and the in-plane transverse (x_2) directions, respectively. However, on the x_1-x_2 plane, both the distribution as well as the orientation of SiC_p are random [Figure 1(b)]. Therefore, it may be assumed that the arrangement of SiC_p is predominantly planar along the extrusion plane.

The example results of the conductivity measurements are shown in Figure 2 for the 2124/SiC/20p. In the figure, the conductivity on the x_1-x_2 plane was found to be greater than that on the x_1-x_3 or x_2-x_3 plane. Moreover, the conductivities on the x_1-x_3 and x_2-x_3 planes appear to be comparable. Therefore, the composite extrusions exhibit anisotropic conductivities, i.e., the conductivity on the x_1-x_2 plane is greater than that on the other orthogonal planes (x_1-x_3 and x_2-x_3 planes). The anisotropic conductivity can be related to the anisotropic orientation distribution of SiC_p, as presented in Figure 1. The different SiC_p orientation distribution between x_1-x_2 and x_1-x_3 (or x_2-x_3) planes (Figure 1) correlates with the different conductivity on these two planes. Moreover, the similar SiC_p orientation distribution on the x_1-x_3 and x_2-x_3 planes corresponds to the comparable conductivity on both planes.

THEORETICAL MODELING

Based on the microstructural characteristics observed in Figure 1, an idealized model for the arrangement of SiC_p may be constructed, as shown in Figure 3. In this arrangement, SiC_p is modeled as a right elliptical cylinder with its axes aligned alternately along the extrusion and in-plane transverse directions, so as to form a crisscross structure. Such an arrangement in Figure 3(b) reflects the extremes of the planar random orientation of SiC_p, as seen on the x_1-x_2 plane [Figure 1(b)], while those in Figures 3(c) and 3(d) represent the preferentially aligned, elongated cross sections in the extrusion and the in-plane transverse directions [Figures 1(c) and 1(d), respectively].

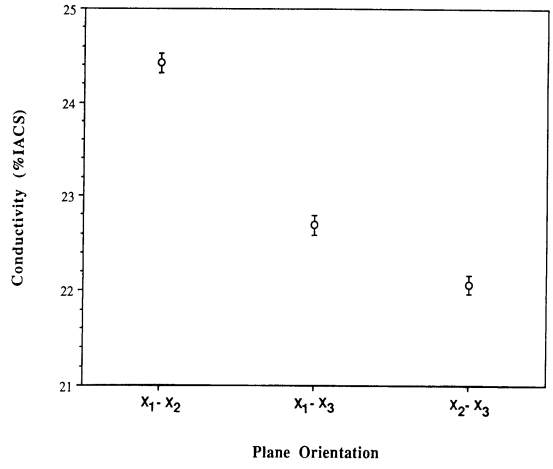

Figure 2. Conductivities of a 2124/SiC/20p composite on the x_1-x_2, x_1-x_3 and x_2-x_3 planes, respectively.

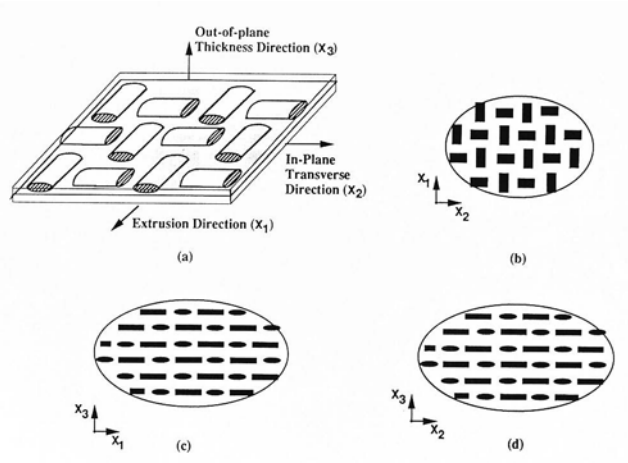

Figure 3. (a) Simplified model for the planar arrangement of SiC_p, (b) - (d) Model representations for the SiC_p cross sections on the x_1-x_2,x_1-x_3 and x_2-x_3 planes, respectively.

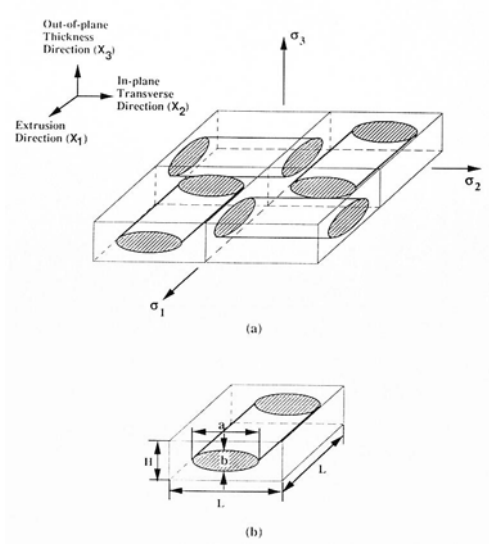

Figure 4. (a) Schematic of the theoretical model showing the assemblage of unit cells for the composite, (b) Representative unit cell consisting of a right elliptical cylinder (SiC_p) in a rectangular box.

In Figure 4(a), the composite is modeled as being composed of the unit cells. A representative unit cell for the idealized regular arrangement is presented in Figure 4(b). The unit cell consists of a rectangular box, in the center of which is placed a SiC_p, right elliptical and cylindrical in shape. The cross sectional dimensions of a unit cell are defined as: "a" and "b" are the major and minor axes of the elliptical cross section of SiC_p, and L is the length of the square base of the unit cell [Figure 4(b)]. The height, H, of the box can be related to the base size, L, and the elliptical cross section of the reinforcement particle by making use of the fact that the SiC_p cross sections are distributed uniformly and randomly, but are oriented preferentially on the x_1-x_3 and x_2-x_3 planes. For an equispaced two-dimensional array of ellipses, the unit cell is a rectangle with the length to height ratio equal to the major axis to minor axis ratio of the ellipse. This trend suggests that the box base length to height ratio, L/H, must equal the SiC_p cross sectional axes ratio, a/b, i.e.,

$$\frac{L}{H} = \frac{a}{b} \qquad (1)$$

The box and the SiC_p sizes can now be interrelated in terms of the volume percentage (v) of SiC_p, which is simply the ratio of the right elliptical cylinder volume to the rectangular box volume. From the definition of the volume fraction, and using Equation (1), the following equations can be obtained:

$$v = \frac{\pi}{4}\left(\frac{b}{H}\right)^2 \quad \text{or} \quad \frac{H}{b} = \frac{L}{a} = \sqrt{\frac{\pi}{4v}} \qquad (2)$$

In the idealized model, Figures 4(b) and 5(a), since SiC_p extends all along the length, L, of the unit cell, the problem of determining the conductivities of the three-dimensional cell [Figure 5(a)] is reduced to that of evaluating the conductivities of a two-dimensional cell shown in Figure 5(b). Moreover, by virtue of the fact that L/H = a/b (Equation 1), the two-dimensional cell in Figure 5(b), which consists of an ellipse within a rectangle, under a geometric scaling with respect to the sides of the rectangle (i.e., scaling the x_2-coordinate with respect to L and the x_3-coordinate with respect to H), reduces to the two-dimensional arrangement of a circle within a unit square cell. This transformation is shown schematically in Figures 5(b)-(c). This transformation was adopted so as to be able to obtain analytical expressions for the composite conductivities, as will be described later.

Behrens formulas [6] for the transverse conductivity may be written in a non-dimensional form as:

$$\frac{\sigma_T}{\sigma_m} = \frac{(\beta + 1) + (\beta - 1)v}{(\beta + 1) - (\beta - 1)v} \qquad (3)$$

where σ_T is the transverse conductivity of the square cell [Figure 5(c)], σ_m denotes the conductivity of the matrix (base alloy), β equals the reinforcement particle (fiber) to matrix conductivity ratio, and v is the reinforcement particle (fiber) volume fraction.

The longitudinal conductivity [σ_L in Figure 5(c)] is given by a volume average of the reinforcement particle and the matrix conductivities, and can be expressed in the following dimensionless form.

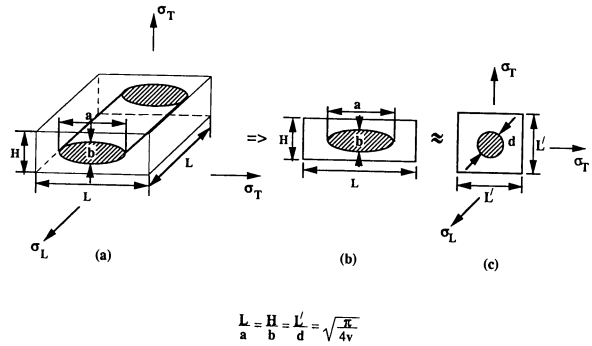

$$\frac{L}{a} = \frac{H}{b} = \frac{L'}{d} = \sqrt{\frac{\pi}{4v}}$$

Figure 5. Transformation of the three-dimensional unit cell to a two-dimensional cell [(a) to (b)], and subsequently to a two-dimensional square cell with an enclosed circular reinforcement particle [(b) to (c)].

$$\frac{\sigma_L}{\sigma_m} = 1 + (\beta - 1)v \qquad (4)$$

Equations 3 and 4 are also the transverse and longitudinal conductivity ratios with respect to the matrix conductivity, respectively, of the three-dimensional rectangular unit cell [Figure 5(a)] in the analysis.

The effective conductivity of the particulate reinforced composite can be evaluated using the unit cell conductivities, by considering an assemblage of unit cells, as shown in Figure 4(a). The idealized arrangement in Figure 3(a) can be constructed using the exact replicas of the assemblage in Figure 4(a). The total resistance (electrical, thermal, etc.) along the x_1 and the x_2 directions is a series combination of the transverse and the longitudinal resistances of the rectangular unit cell [Figures 4(b) and 5(a)]. Therefore, the effective conductivity in the extrusion or the in-plane transverse direction, σ_1 or σ_2, respectively [Figure 4(a)], is a harmonic average of the transverse and longitudinal conductivities (Equations 3 and 4). In a dimensionless form, it may expressed as:

$$\frac{\sigma_1}{\sigma_m} = \frac{\sigma_2}{\sigma_m} = \frac{2\left(\frac{\sigma_T}{\sigma_m}\right)\left(\frac{\sigma_L}{\sigma_m}\right)}{\left(\frac{\sigma_T}{\sigma_m}\right) + \left(\frac{\sigma_L}{\sigma_m}\right)} \qquad (5)$$

In Figure 4(a), the conductivity of the assemblage in the out-of-plane thickness direction (σ_3) equals the transverse conductivity of the unit cell (Equation 3). i.e.,

$$\frac{\sigma_3}{\sigma_m} = \frac{\sigma_T}{\sigma_m} \qquad (6)$$

In the experiments, a circular eddy current probe was used in the measurements of conductivities. The measured values were, thus, an average of the conductivities along several directions spanning the entire plane. Thus, in order to be able to compare the model results with the experimental values, it is necessary to determine the planar conductivities for each of the three planes, x_1-x_2, x_1-x_3 and x_2-x_3 in Figure 4(a). In the present simplified model, the planar conductivity is calculated by averaging the conductivities along two orthogonal directions defining the plane. Thus, the three planar conductivities, $\sigma_{1\text{-}2}$, $\sigma_{1\text{-}3}$, and $\sigma_{2\text{-}3}$, scaled with respect to the matrix conductivity, σ_m, can be expressed as:

$$\frac{\sigma_{1\text{-}2}}{\sigma_m} = \frac{1}{2}\left(\frac{\sigma_1}{\sigma_m} + \frac{\sigma_2}{\sigma_m}\right) \qquad (7)$$

$$\frac{\sigma_{1\text{-}3}}{\sigma_m} = \frac{\sigma_{2\text{-}3}}{\sigma_m} = \frac{1}{2}\left(\frac{\sigma_1}{\sigma_m} + \frac{\sigma_3}{\sigma_m}\right) \qquad (8)$$

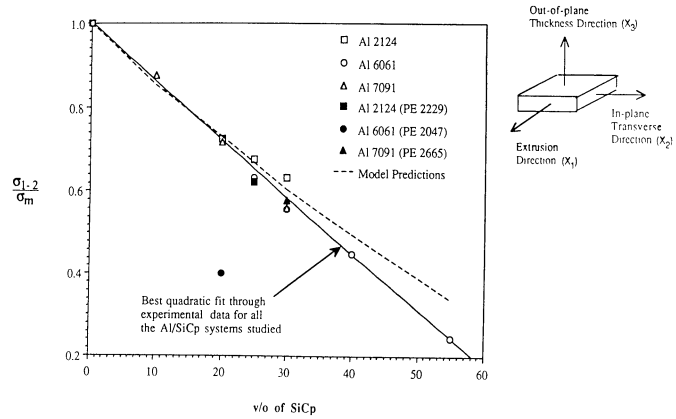

Figure 6. Comparisons of measured and theoretically predicted conductivity ratios on the x_1-x_2 plane.

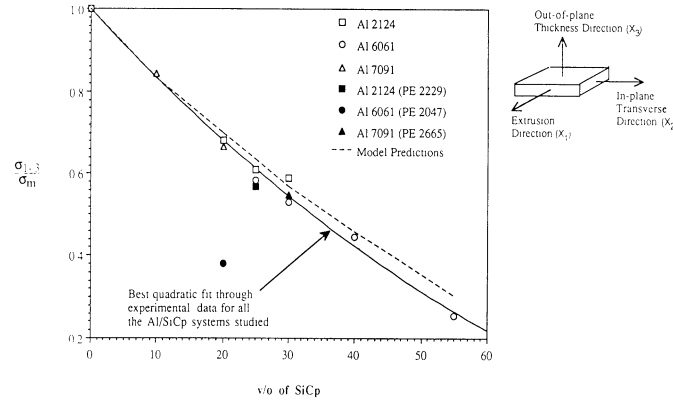

Figure 7. Comparisons of measured and theoretically predicted conductivity ratios on the x_1-x_3 plane.

DATA COMPARISONS AND DISCUSSION

Figures 6-7 show the comparisons between the theoretical planar conductivity ratios (Equations 7 and 8) and the experimental values, for all the composite systems investigated. The experimental data on the planar conductivities were cast into a non-dimensional form ($\sigma_{1\text{-}2}/\sigma_m$ and $\sigma_{1\text{-}3}/\sigma_m$) by normalizing with respect to the conductivity of the corresponding base alloy on the respective plane. In the figure, the present model predictions are shown by dashed lines, while the symbols are the experimental data for the three composite systems. The solid line denotes the best fit curve through the experimental data. Note that in the model prediction, the value of β is set to be 0.0026 [7]. It is evident from Figure 6 that on the x_1-x_2 plane, the theoretical predictions and the experimental data compare very well, to within about 8%, for the SiC_p volume fractions less than or equal to about 35%. For higher volume fractions, the present model is seen to over-predict the conductivities. This trend can be attributed to the assumption of the planar arrangement in the model, which neglects the resistance due to SiC_p's present in between planes. The effect is more pronounced for the higher volume fractions since, due to the closer packing, there may be more out-of-plane SiC_p's.

On the x_1-x_3 plane (Figures 7), the conductivities predicted by the present model show excellent agreement, to within 5%, with the experimental measurements over almost the entire range of SiC_p volume fractions from 0 to 55%. The differences between the model predictions and the experimental data may be ascribed to the following three factors namely, (a) the assumption of the uniform-random arrangement of SiC_p, (b) the approximation in calculating the planar conductivities, and (c) the presence of intermetallic compounds in the composites [2], which are neglected in the simplified model.

CONCLUSIONS

Eddy current techniques were used to determine the electrical conductivities of silicon-carbide-particulate (SiC_p) reinforced aluminum MMCs. The composites investigated included 2124, 6061 and 7091 aluminum alloys reinforced by SiC_p. The volume percentage of SiC_p covered a wide range from 0 to 55 %. The composites demonstrated anisotropic conductivity with the maximum conductivity occurring along the extrusion plane. Microstructural analyses revealed that the observed anisotropic conductivity could be related to the preferred orientation distribution of SiC_p. A theoretical model including the effects of composite constituents (aluminum matrix alloy and SiC_p) was developed to estimate the anisotropic conductivities of the composites. The theoretical predictions of conductivities were found to be in good agreement with the experimental results.

REFERENCES

1. G. Mott and P. K. Liaw, Metallurgical Transactions A, vol. 19A, 1988, p. 2233.
2. P. K. Liaw, R. E. Shannon, W. G. Clark, Jr. and W. C. Harrigan, Jr., Morris E. Fine Symposium, TMS-AIME, P. K. Liaw, J. R. Weertman, H. L. Marcus and J. S. Santner, eds., 1991, p. 193.
3. H. Jeong, D. K. Hsu, R. E. Shannon and P. K. Liaw, Morris E. Fine Symposium, TMS-AIME, P. K. Liaw, J. R. Weertman, H. L. Marcus and J. S. Santner, eds., 1991, p. 209.
4. H. Jeong, D. K. Hsu, R. E. Shannon and P. K. Liaw, Symposium on "Nondestructive Evaluation and Material Properties of Advanced Materials", TMS-AIME, P. K. Liaw, O. Buck and S. M. Wolf, eds., 1991, p. 37.
5. R. E. Shannon, P. K. Liaw and W. C. Harrigan, Jr., Metallurgical Transactions A, vol. 23A, 1992, p. 1541.
6. E. Behrens, Journal of Composite Materials, vol. 2, 1968, p. 2.
7. R. C. Marshall, J. W. Faust, Jr., and C. E. Ryan, eds., Silicon Carbide-1973, University of South Carolina Press, Columbia, SC, 1974, p. 673.